# Subband spectroscopy of single and coupled GaAs quantum wells

A. Lorke* and U. Merkt
*Institut für Angewandte Physik, Universität Hamburg, Jungiusstrasse 11, D-2000 Hamburg 36, West Germany*

F. Malcher†
*Institut für Theoretische Physik, Universität Regensburg, Universitätsstrasse 31, D-8400 Regensburg, West Germany*

G. Weimann
*Walter-Schottky-Institut der Technischen Universität München, D-8046 Garching bei München, West Germany*

W. Schlapp
*Forschungsinstitut der Deutschen Bundespost, Postfach 5000, D-6100 Darmstadt, West Germany*
(Received 26 February 1990)

Electronic excitations in the conduction band of a single-side-doped GaAs quantum well with a thin AlAs barrier in its center (coupled, double quantum well) and of a well of equal width and growth parameters without barrier (single quantum well) are examined by far-infrared Fourier-transform spectroscopy. We measure intersubband energies, cyclotron masses in perpendicular magnetic fields, and dipole matrix elements in tilted magnetic fields. The experimental results are compared for the two samples and are quantitatively reproduced by a self-consistent description that takes into account the nonparabolic band structure of the semiconductors.

## I. INTRODUCTION

Quantum wells and compositional superlattices on GaAs play a major role in research and application of artificial semiconductor structures because their electronic properties can be exploited for a wide range of applications, thus permitting the design of sophisticated devices.[1] Coupled, double quantum wells (CDQW's), which consist of two GaAs quantum wells separated by a thin AlAs barrier, may be considered the simplest building block of superlattices and hence play an important role in fundamental experimental and theoretical studies. In particular, the formation of minibands in a superlattice is a consequence of the coupling of quantized levels in adjacent wells. This coupling is entirely analogous to the situation when atoms bond to molecules. In this context, a CDQW can be regarded as a solid-state analog of the hydrogen molecule. Accordingly, the ground states of the uncoupled wells are energetically split into a lower bonding and a higher-lying antibonding state.

The electronic structure of a CDQW has been studied previously by luminescence excitation spectroscopy[2,3] and by resonant tunneling.[4] Here we directly study the transitions between quantized conduction-band levels with far-infrared Fourier-transform spectroscopy and provide a detailed theoretical analysis that takes into account the nonparabolic band structure of bulk GaAs, $Al_xGa_{1-x}As$, and AlAs. Unlike in the interpretation of luminescence data,[2,3] we need not bother about the complicated hole subband structure. We have the advantage over tunneling experiments[4] that we can carry out measurements at zero bias when there is no external Stark shift and no additional tunneling to contacts.[5] Our theoretical description is substantiated by a comparative study of the CDQW and a corresponding single quantum well (SQW) of equal width.

## II. EXPERIMENTS

The samples are grown by molecular-beam epitaxy (MBE) on semi-insulating GaAs substrates. The deposition starts with a GaAs buffer layer (2 $\mu$m) and an eight period superlattice of ($Al_{0.36}Ga_{0.64}As$/110 Å) (GaAs/35 Å). It is followed by the active well, an $Al_{0.36}Ga_{0.64}As$ spacer (160 Å), Si-doped $Al_{0.36}Ga_{0.64}As$ (400 Å), Si-doped GaAs (35 Å), and an undoped GaAs cap layer (175 Å). The SQW consists of GaAs (145 Å) and the CDQW of two GaAs layers, each of width 72 Å, which are separated by a 3-ML-thick AlAs (8.5 Å) barrier (ML denotes monolayer). For both samples the course of the conduction band in the vicinity of and inside the active wells, as well as the quantized subband energies and the normalized wave functions, are shown in Figs. 1(a) and 1(b).

In order to excite intersubband resonances in a strip-line arrangement,[5,6] the front and back sides of the samples are metallized by 1000-Å-thick aluminum films. The front metallization simultaneously serves as a gate contact that allows one to tune the quasi-two-dimensional 2D electron density $n_s$ in the active wells by the application of a gate voltage $V_g$. The densities are determined from the Shubnikov–de Haas oscillations of the static conductivity.[7] In the dark and at bias $V_g=0$, we obtain the densities $n_s=3.9\times10^{11}$ and $2.8\times10^{11}$ cm$^{-2}$ for the SQW and CDQW, respectively.

The optical experiments are performed with a rapid-scan Fourier-transform spectrometer in the far-infrared regime at liquid-helium temperatures ($T\cong2$ K). The metallization and the strip-line arrangement sketched in

 

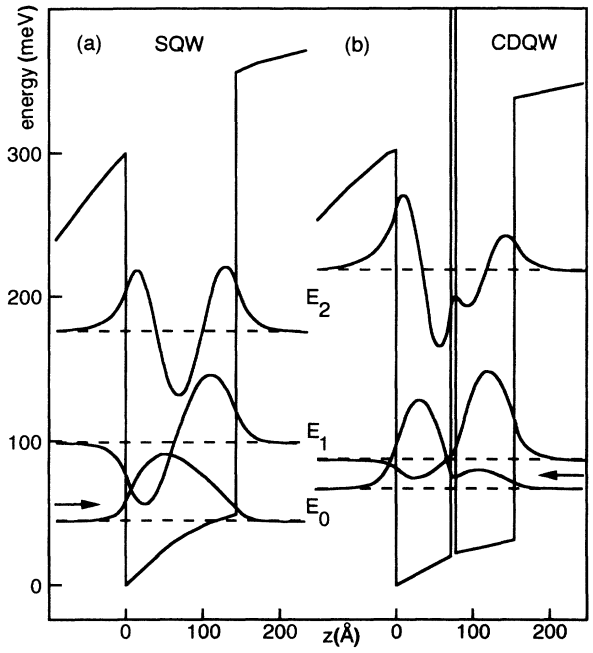


FIG. 1. Calculated self-consistent subband wave functions, energies, and interface potentials for (a) the SQW ($n_s = 3.9\times10^{11}$ cm$^{-2}$, 145 Å) and (b) the CDQW ($n_s = 2.8\times10^{11}$ cm$^{-2}$, 152 Å).

the inset of Fig. 2 guarantee the proper light polarization parallel to the growth direction. This polarization allows direct excitation of intersubband transitions between the quantized well levels. Cyclotron resonance is studied using a sample holder which, *in situ*, allows one to vary the angle $\theta$ between surface normal and magnetic field direction in a superconducting solenoid. In these experiments the samples are not metallized and the infrared radiation passes through their front sides. When a sample is tilted with respect to the magnetic field direction, the light polarization still is essentially parallel to the 2D electron

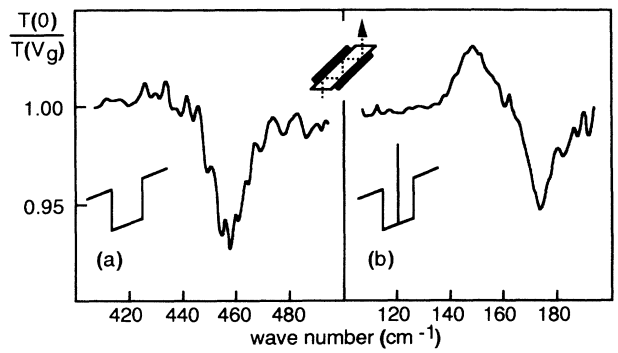


FIG. 2. Relative transmittance spectra for (a) the SQW and (b) the CDQW. Reference voltages for the SQW and CDQW are $V_g = -1.5$ and $-0.75$ V, respectively. The CDQW is not completely depleted at $-0.75$ V, and hence the related Stark-shifted resonance appears as a maximum at a wave number $143\pm2$ cm$^{-1}$.

layer. This results from the high dielectric functions of the semiconductors that cause the light to be refracted into the growth direction. Low-noise detection of transmittance signals $T$ is achieved by recording the ratios $T(V_g=0)/T(V_g)$ and $T(B=0)/T(B)$ in the case of intersubband and cyclotron resonances, respectively.[8]

Intersubband resonances for both samples are shown in Fig. 2. In the SQW a negative gate voltage, $V_g = -1.5$ V, completely depletes the well of electrons, and only the intersubband resonance for zero bias, $V_g = 0$, at a wave number $458\pm2$ cm$^{-1}$ is observed in the spectrum. For the CDQW both resonances for voltages $V_g = -0.75$ V and $V_g = 0$ are visible. Because of electric breakthrough of the insulating GaAs cap layer, we could not apply more negative voltages to deplete this sample. However, the resonance at the lower voltage is sufficiently shifted away to a lower wave number, $143\pm3$ cm$^{-1}$, by the Stark effect[2,3,5] to allow for a precise determination of the resonance position, $173\pm2$ cm$^{-1}$, for zero bias. Whereas the widths [full width at half maximum (FWHM)] of the intersubband resonances for the SQW ($\simeq 15$ cm$^{-1}$) and CDQW ($\simeq 11$ cm$^{-1}$) are similar, those of cyclotron resonance are markedly different. Taking into account saturation effects of the cyclotron resonances,[9] we deduce mobilities 350 000 and 150 000 cm$^2$ V$^{-1}$ s$^{-1}$ for the SQW and CDQW, respectively, at magnetic field strengths of $B \simeq 8$ T. The reduced mobility in the CDQW may be explained by scattering at the two additional interfaces of the AlAs barrier.

## III. THEORY

The theoretical description follows Ref. 10 and starts from an effective $2\times2$ subband Hamiltonian $H = H_0 + H_1$ that contains the Hamiltonian in the parabolic approximation,

$$H_0 = -\frac{\hbar^2}{2}\partial_z \frac{1}{m^*(z)}\partial_z + \frac{\hbar^2 k_\parallel^2}{2m^*(z)} + U(z) , \qquad (1)$$

where the coordinate $z$ is in the growth direction, $\mathbf{k}_\parallel = (k_x, k_y)$ is the momentum parallel to the electron layer, and $U(z)$ is the total interface potential. Deviations from the parabolic approximation due to higher-order terms in the electron momentum as well as in the magnetic and electric field are written in terms of invariants and summarized in

$$H_1(\mathbf{k},\mathbf{E},\mathbf{B}) = \sum_{\kappa,\lambda} a_{\kappa\lambda} \sum_L X_L^{(\kappa,\lambda)} K_L^{(\kappa,\lambda)*}(\mathbf{k}_\parallel,\mathbf{E},\mathbf{B}) . \qquad (2)$$

They are composed of the Pauli spin matrices $X_\alpha^{(4)} = \sigma_\alpha$ ($\alpha = x,y,z$), the $2\times2$ unit matrix $X_1^{(1)}$, and irreducible tensor components $K_L^{(\kappa,\lambda)}$. The latter are functions of the electron wave vector $\mathbf{k}_\parallel$, the electric field $\mathbf{E} = (0,0,-(1/e)\partial_z U)$, and the magnetic field $\mathbf{B} = (0,0,B)$. They transform according to the irreducible representation $\Gamma_\kappa$ of the zinc-blende-structure point group $T_d$. Starting from a $\mathbf{k}\cdot\mathbf{p}$ approach in the vicinity of the $\Gamma$ point, the nonparabolic part, $H_1$, can be obtained in an equivalent way by reducing the $14\times14$ bulk Hamiltonian, which considers the coupling of the lowest GaAs

conduction band to the valence bands and to higher conduction bands by fourth-order perturbation theory.[11] Thus the expansion coefficients $a_{\kappa\lambda}$ can be expressed by momentum matrix elements and energy gaps at the $\Gamma$ point, which are well known for GaAs, AlAs, and $Al_xGa_{1-x}As$.[12] Because the conduction-band minimum of AlAs at the $X$ point is eventually[12] only about 150 meV above the $\Gamma$-point minimum of GaAs, one might expect the $X$-point minimum to influence the subband states. However, the $X$-point minimum of GaAs (460 meV above the $\Gamma$ point) forms a barrier for the $X$-point states of AlAs. States confined in this narrow well have subband energies above the subband states derived here for the $\Gamma$ point. Therefore we expect no influence from the $X$ point.

The eigenvalue problem described by the Hamiltonian $H_0$ is solved self-consistently together with Poisson's equation for the Hartree potential determined by the charge distribution in the quantum wells. The total potential $U(z)$ in Eq. (2) consists of the Hartree potential, a parameterized exchange-correlation potential,[13] and a steplike potential. The latter considers the sample geometry and accounts for the $\Gamma$-point offsets 0.30 and 1.05 eV of the conduction band at the $GaAs/Al_xGa_{1-x}As$ and GaAs/AlAs interfaces, respectively. These offsets are 65% of the energy-gap difference between GaAs and $Al_xGa_{1-x}As$.[14]

The potential is also influenced by the depletion charge, which leads to asymmetric bottoms of the wells and to internal Stark effects. The detailed value of the depletion charge density $N_d$ has only little influence on the calculated results. Experimentally, it is not precisely known and we take $N_d=7.0\times10^{10}$ cm$^{-2}$ for both samples. This value is consistent with the unintentional background doping measured with the van der Pauw method on thick, nominally undoped GaAs layers, as well as with results of intersubband resonance experiments on heterojunctions grown under the same conditions.[15] Self-consistently calculated subband wave functions $\xi_i(z)$, subband energies $E_i$ and interface potentials $U(z)$ for the SQW and CDQW are shown in Figs. 1(a) and 1(b). Numerical values for subband separations $E_{i0}$ and dipole matrix elements $z_{i0}=\langle\xi_i(z)|z|\xi_0(z)\rangle$ are given in Table I. Comparison with intersubband resonance data, $\tilde{E}_{10}$, requires the calculation of the depolarization shift $\tilde{E}_{10}-E_{10}$. Applying the model introduced by Ando[7] for 2D inversion layers on Si to the present structures, the calculated values $\tilde{E}_{10}$ are in good agreement with the experimental ones.

In magnetic fields, Landau levels of the lowest subband are determined by a variational calculation using the function

$$\Phi=\xi_0(z)\sum_{N,s}c_{Ns}|Ns\rangle\ , \tag{3}$$

with spin projections $s$ and minimizing the expectation value of $H_1$ with respect to the coefficients $c_{Ns}$ numerically. From the Landau energies $E_{N,s}$ the usual cyclotron masses

$$m^*=\frac{e\hbar B}{E_{N+1,s}-E_{N,s}} \tag{4}$$

are calculated. Since spin splitting is not resolved in our spectra, we average the cyclotron masses over the spin projections $s=\pm\frac{1}{2}$ for comparison with experimental values.

## IV. DISCUSSION AND CONCLUSIONS

Figure 3 shows the comparison of experimental and theoretical cyclotron masses in magnetic fields which are applied perpendicularly to the well layers ($\theta=0°$). Mainly as a result of band nonparabolicity and only to a minor extent as a consequence of the small probability density in the $Al_{0.36}Ga_{0.64}As$ ($m_0^*=0.096m_e$) or AlAs ($m_0^*=0.15m_e$), the cyclotron masses exceed the value $m_0^*=0.0665m_e$ at the GaAs conduction-band edge. Also as a result of nonparabolicity, the masses increase with increasing magnetic field strength in the magnetic quantum limit for filling factors $\nu=hn_s/eB<2$. The theoretical lines are calculated for Landau transitions $N=0\rightarrow1$ and $1\rightarrow2$ and are drawn in the regime of filling factors where they can contribute to the signals. There is good agreement between the experimental masses and their theoretical description that does not contain any adjustable parameter. However, in the spectra the Landau transitions $0\rightarrow1$ and $1\rightarrow2$ are unresolved in both samples. For the CDQW a slight mass oscillation is observable below $B\simeq8$ T that may be of similar origin as the anomalies close to filling factors $\nu=2$ that previously have been observed in GaAs heterojunctions.[16] These anomalies may also explain the observation that the in-

TABLE I. Self-consistently calculated and experimentally determined results for an $Al_{0.36}Ga_{0.64}As/GaAs$ SQW ($n_s=3.9\times10^{11}$ cm$^{-2}$, 144 Å) and a CDQW ($n_s=2.8\times10^{11}$ cm$^{-2}$, 152 Å) with a 3-ML-thick AlAs (8.5 Å) barrier in its center. Experimental errors of intersubband energies $\tilde{E}_{10}$ and matrix elements $z_{10}$ are about 0.3 meV and 2 Å, respectively.

| | SQW | | CDQW | |
|---|---|---|---|---|
| | Theor. | Expt. | Theor. | Expt. |
| $E_{10}$ (meV) | 52.7 | | 21.0 | |
| $E_{20}$ (meV) | 130 | | 148 | |
| $\tilde{E}_{10}$ (meV) | 56.2 | 56.8 | 21.6 | 21.4 |
| $z_{10}$ (Å) | 31.3 | 33.0 | 21.0 | 20.0 |
| $z_{20}$ (Å) | 2.5 | | 13.9 | |

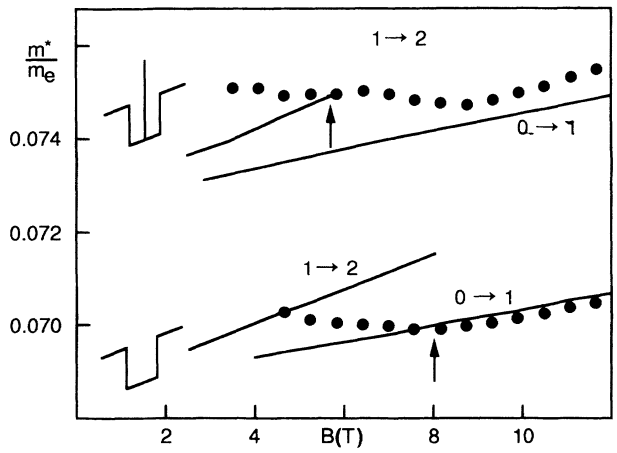


FIG. 3. Experimental and calculated cyclotron masses for Landau transitions $0\rightarrow 1$ and $1\rightarrow 2$. The arrows indicate the position of filling factors $\nu=2$ as obtained from Shubnikov–de Haas measurements.

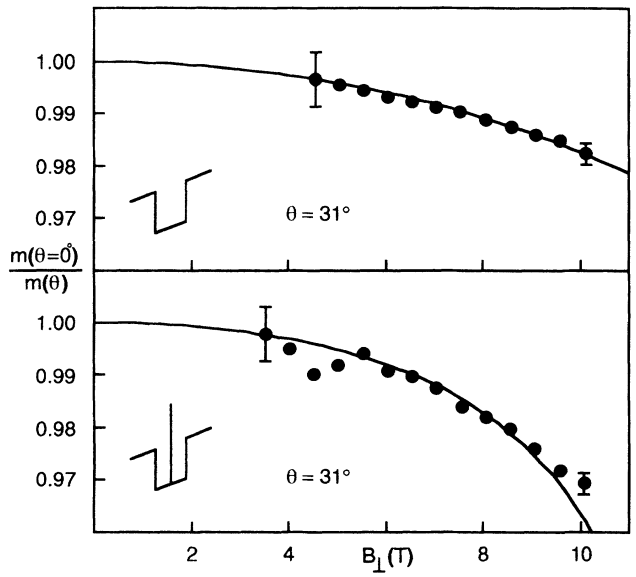


FIG. 4. Mass ratios obtained from cyclotron resonance in perpendicular and tilted magnetic fields as a function of the magnetic field component perpendicular to the 2D electron layer. The solid lines are calculated from Eq. (5) using the theoretical matrix elements of Table I.

crease of the cyclotron mass, which is indicative of the magnetic quantum limit ($\nu<2$), starts only at magnetic fields $B\simeq 8$ T.

Table I also gives the theoretical dipole matrix elements $z_{10}$ and $z_{20}$. In order to verify their values, we have measured cyclotron resonance in tilted magnetic fields.[17] As long as the cyclotron energy $\hbar\omega_{c\perp}=\hbar eB_\perp/m^*$ of the magnetic field component $B_\perp$ perpendicular to the well layers is smaller than the subband spacing $E_{10}$, perturbation theory is valid and predicts an apparent angle-dependent mass $m^*(\theta)$ that obeys the relation[15,17]

$$\frac{m^*(\theta=0°)}{m^*(\theta)}=1-\tan^2\theta\sum_{i>0}\frac{m^* z_{i0}^2 E_{io}}{\hbar^2}\frac{(\hbar\omega_{c\perp}/E_{io})^2}{1-(\hbar\omega_{c\perp}/E_{i0})^2} \tag{5}$$

in the lowest electric subband. Mass ratios according to Eq. (5) are presented in Fig. 4 as functions of the perpendicular magnetic field component $B_\perp$ at a fixed tilt angle $\theta$. The contribution of the adjacent subband $i=1$ is dominant to a high degree and one can ignore higher terms ($i>1$) in the sum of Eq. (5). This way the experimental matrix elements $z_{10}$ in Table I are determined. The solid lines in Fig. 4 are calculated from Eq. (5) using the theoretical energies $E_{i0}$ and matrix elements $z_{i0}$ ($i=1,2$) of Table I. Perturbation theory describes the experimental data very well, except for few data points for the CDQW at field components $B_\perp\simeq 4$ and 10 T. There, the deviations from Eq. (5) are caused by the mass anomaly discussed above and by the influence of the full-field coupling,[15] respectively.

Equation (5) does not take into account many-electron and nonparabolicity effects. However, the influence of these effects on the apparent angle-dependent mass is estimated to be less than the size of the corresponding error bars in Fig. 4. Also, the contribution of states $i>2$ in the sum of Eq. (5) is negligible.

In conclusion, we have measured subband energies, dipole matrix elements, and effective masses of electrons in a SQW and in a CDQW with uncertainties of only few percent. Without any adjustable parameter, a self-consistent theoretical description that takes into account the nonparabolic band structure explains the experimental values within their errors. In the CDQW the nonparabolicity of GaAs brings about a significant increase of the effective mass $m^*\simeq 0.075m_e$ for the motion parallel to the electron layer. The higher mass, $m^*=0.150m_e$, of AlAs does not appreciably contribute to this increase over the GaAs mass, $m^*=0.0665m_e$, at the conduction-band edge. This demonstrates that thin tunneling barriers at fixed GaAs quantum-well widths not only allow one to tune energy levels and dipole matrix elements, but also the effective mass, in an astonishingly wide range. Our results also confirm that only $\Gamma$-point-related states need to be considered in the description of AlAs barriers in GaAs quantum wells at modest electric field strengths.[18] Unlike for resonant tunneling in double-barrier heterostructures,[19] $X$-point levels do not contribute measurably.

## ACKNOWLEDGMENTS

We thank J. P. Kotthaus and U. Rössler for valuable discussions and the Deutsche Forschungsgemeinschaft (Bonn, Germany) for financial support.

*Present address: Sektion Physik der Ludwig-Maximilians-Universität München, Geschwister-Scholl-Platz 1, D-8000 München 22, West Germany.

†Present address: Linde A. G., D-8023 Höllriegelskreuth, West Germany.

[1]L. Esaki, in *Physics and Applications of Quantum Wells and Superlattices,* edited by E. E. Mendez and K. von Klitzing (Plenum, New York, 1987), pp. 1–19.

[2]S. R. Andrews, C. M. Murray, R. A. Davies, and T. M. Kerr, Phys. Rev. B **37**, 8198 (1988).

[3]J. Lee, M. O. Vassell, E. S. Koteles, and B. Elman, Phys. Rev. B **39**, 10 133 (1989).

[4]Y. Zohta, T. Nozu, and M. Obara, Phys. Rev. B **39**, 1375 (1989).

[5]A. Lorke, A. D. Wieck, U. Merkt, G. Weimann, and W. Schlapp, Superlattices Microstruct. **5**, 279 (1989).

[6]A. D. Wieck, K. Bollweg, U. Merkt, G. Weimann, and W. Schlapp, Phys. Rev. B **38**, 10 158 (1988).

[7]T. Ando, A. B. Fowler, and F. Stern, Rev. Mod. Phys. **54**, 437 (1982).

[8]E. Batke and D. Heitmann, Infrared Phys. **24**, 189 (1984).

[9]F. Thiele, W. Hansen, M. Horst, J. P. Kotthaus, J. C. Maan, U. Merkt, K. Ploog, G. Weimann, and A. D. Wieck, in *High Magnetic Fields in Semiconductor Physics,* Vol. 71 of *Springer Series in Solid State Sciences,* edited by G. Landwehr (Springer, Heidelberg, 1987), pp. 252–255.

[10]F. Malcher, G. Lommer, and U. Rössler, Superlatt. Microstruct. **2**, 267 (1986); **2**, 273 (1986).

[11]M. Braun and U. Rössler, J. Phys. C **18**, 3365 (1985).

[12]*Landolt-Börnstein, Numerical Data and Functional Relationships in Science and Technology,* Series III, edited by O. Madelung (Springer, Berlin, 1982), Vol. 17a; Vol. 22a (1987).

[13]L. Hedin and B. I. Lundquist, J. Phys. C **4**, 2064 (1971).

[14]U. Rössler, Solid State Commun. **65**, 1279 (1988).

[15]A. D. Wieck, F. Thiele, U. Merkt, K. Ploog, G. Weimann, and W. Schlapp, Phys. Rev. B **39**, 3785 (1989).

[16]R. J. Nicholas, M. A. Hopkins, D. J. Barnes, and M. A. Brummell, H. Sigg, D. Heitmann, K. Ensslin, J. J. Harris, C. T. Foxon, and G. Weimann, Phys. Rev. B **39**, 10 955 (1989).

[17]S. Oelting, A. D. Wieck, E. Batke, and U. Merkt, Surf. Sci. **196**, 273 (1988).

[18]M.-H. Meynadier, R. E. Nahory, J. M. Worlock, M. C. Tamargo, J. L. de Miguel, and M. D. Sturge, Phys. Rev. Lett. **60**, 1338 (1988).

[19]A. R. Bonnefoi, T. C. McGill, and R. D. Burnham, Phys. Rev. B **37**, 8754 (1988).